

Contents

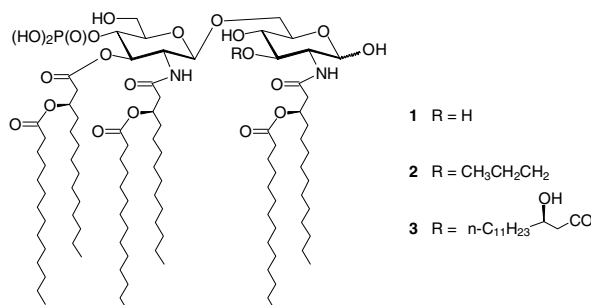
RAPID COMMUNICATION

- Relationship between structure and three-bond proton–proton coupling constants in glycosaminoglycans** pp 779–783
M. Hricovini* and F. Bízík

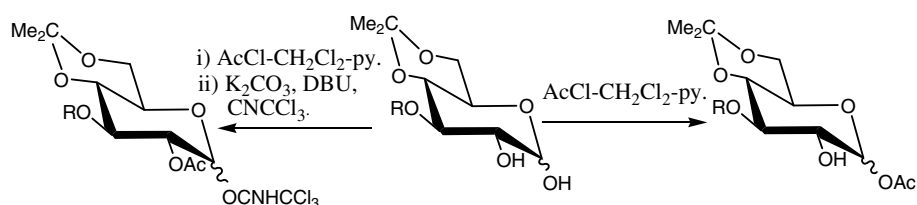
3D Structures and three-bond proton–proton spin–spin coupling constants ($^3J_{\text{H-C-C-H}}$) were determined using theoretical methods in various glycosaminoglycan (GAG) molecules. The computed $^3J_{\text{H-C-C-H}}$ values showed a strong dependence on the molecular geometry. This dependence was expressed in a simple analytical form relating $^3J_{\text{H-C-C-H}}$ and torsion angles in GAGs:
 $^3J_{\text{H-C-C-H}} = 9.6 \cos^2 \phi - 0.6 \cos \phi + 0.2$.

FULL PAPERS

- Monophosphoryl lipid A analogues with varying 3-O-substitution: synthesis and potent adjuvant activity** pp 784–796
Zi-Hua Jiang,* Wladyslaw A. Budzynski, Dongxu Qiu, Damayanthi Yalamati and R. Rao Koganty*



- Regio- and stereoselective anomeric esterification of glucopyranose 1,2-diols and a facile preparation of 2-O-acetylated glucopyranosyl trichloroacetimidates from the corresponding 1,2-diols** pp 797–805
Jianjun Zhang, Xiaomei Liang, Daoquan Wang* and Fanzuo Kong



pp 806–818

9 D-*arabino*
10 D-*lyxo*
11 D-*ribo*
12 D-*xylo*
 1-(*R*) Series

13 D-*arabino*
14 D-*lyxo*
15 D-*ribo*
16 D-*xylo*
 1-(*S*) Series

17 D-*arabino*
18 D-*lyxo*
19 D-*ribo*
20 D-*xylo*

21 D-*arabino*
22 D-*lyxo*
23 D-*ribo*
24 D-*xylo*

pp 819–825

The crystal transformation of dihydrate trehalose to anhydrous trehalose was investigated using ethanol and a new type of crystal particle with porous structure could be obtained. The crystal transformation was monitored by measuring the crystal moisture content.

pp 826–834

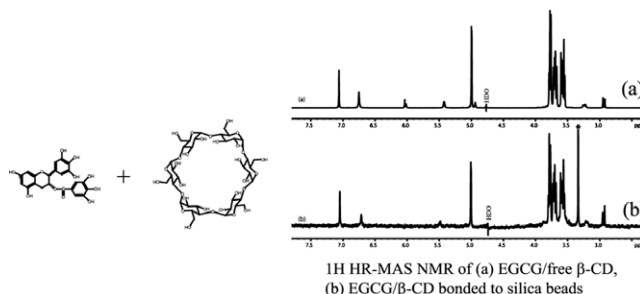
Figure 1 consists of three parts. The top left shows the chemical structure of poly(2-vinylpyridine) labeled 'STRUCTURE I', with protons labeled 2^{H}N_1 through 6^{H}N_1 . The top right shows the same polymer labeled 'STRUCTURE II', with protons labeled 2^{H}N_2 through 6^{H}N_2 . The bottom part is a ^1H NMR spectrum of the polymer in CDCl_3 . The x-axis is chemical shift in ppm, ranging from 0 to 9. The y-axis is relative intensity from 0 to 100. The spectrum shows several sharp peaks: a small peak at ~0.9 ppm (2^{H}N_1), a large peak at ~1.8 ppm (3^{H}N_1), a peak at ~2.1 ppm (4^{H}N_1), a very large peak at ~2.3 ppm (5^{H}N_1), a peak at ~2.5 ppm (6^{H}N_1), a small peak at ~3.1 ppm (2^{H}N_2), a small peak at ~3.3 ppm (3^{H}N_2), a small peak at ~3.5 ppm (4^{H}N_2), a small peak at ~3.7 ppm (5^{H}N_2), and a small peak at ~3.9 ppm (6^{H}N_2).

pp 835–842

Chemical reaction scheme showing the degradation of a disaccharide derivative. The reactant is a disaccharide with a carboxylate group (COO⁻) and a sulfonate group (CH₂OSO₃⁻). It reacts with NaOH at 40 °C for 16 hours to produce three products: a disaccharide with a carboxylate group (COO⁻) and a sulfonate group (CH₂OSO₃⁻), a disaccharide with a carboxylate group (COO⁻) and a sulfonate group (CH₂OSO₃⁻), and a disaccharide with a carboxylate group (COO⁻) and a sulfonate group (CH₂OSO₃⁻).

NMR Studies on the interaction between (–)-epigallocatechin gallate and cyclodextrins, free and bonded to silica gels pp 843–850

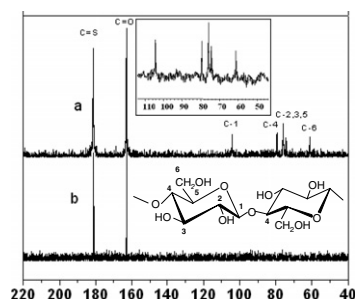
Jun Xu, Tianwei Tan,* Jan-Christer Janson, Lennart Kenne and Corine Sandström*



Direct dissolution of cellulose in NaOH/thiourea/urea aqueous solution pp 851–858

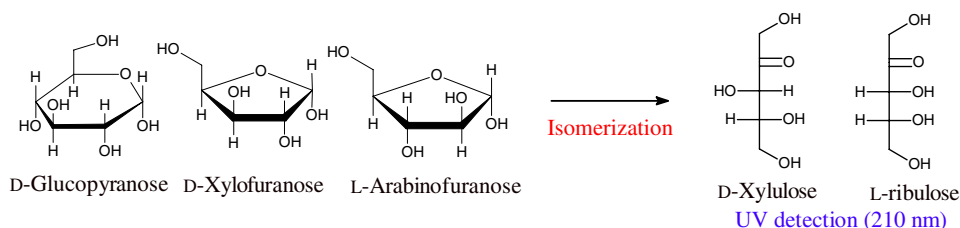
Huajin Jin, Chunxi Zha and Lixia Gu*

The ¹³C NMR spectroscopy shows that the interactions between NaOH and urea, as well as between NaOH and thiourea, play an important role in improving the dissolution of cellulose, and that NaOH, thiourea, and urea were bound to cellulose molecules, which brings cellulose molecules into aqueous solution to a certain extent, and prevents cellulose macromolecules from associating.



Selective ketopentose analysis in concentrate carbohydrate syrups by HPLC pp 859–864

Sebastien Givry,* Christophe Bliard and Francis Duchiron

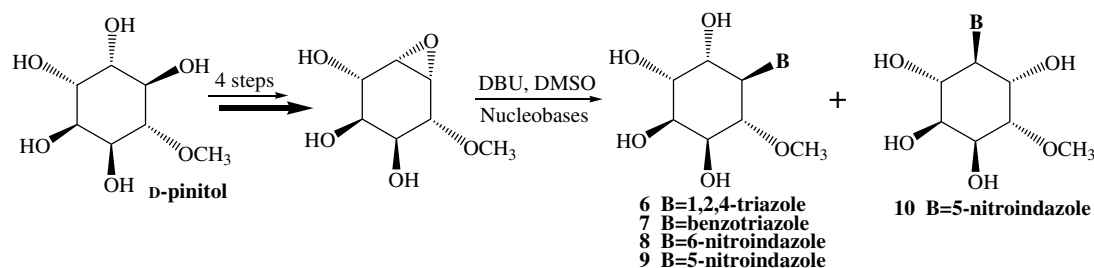


This paper describes a chromatographic method for the detection of low ketose concentrations in a complex syrup containing high concentration of carbohydrates such as glucose and pentoses by UV detection at 210 nm.

NOTES

Synthesis ofazole nucleoside analogues of D-pinitol as potential antitumor agents pp 865–869

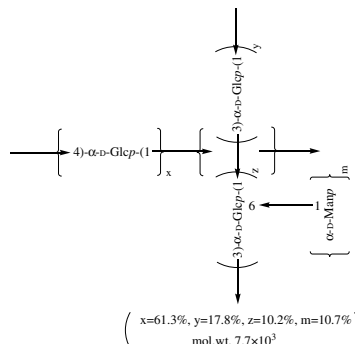
Tianrong Zhan* and Hongxiang Lou



Isolation and characterization of a mannoglucan from edible *Cordyceps sinensis* mycelium

pp 870–875

Yalin Wu, Nan Hu, Yuanjiang Pan,* Lijun Zhou and Xuxia Zhou



*Corresponding author

i* Supplementary data available via ScienceDirect

COVER

The image shows the ball-and-stick representation of a potent *n*-butyl thiazoline inhibitor of *Q*-GlcNAcase, bound in the active centre of the enzyme. The work is the result of collaboration between the groups of Professors David Vocadlo (Simon Fraser University, British Columbia, Canada) and Gideon Davies (University of York, UK). The image, generated with PYMOL (DeLano Scientific LLC, <http://pymol.sourceforge.net/>), shows the observed electron density as a blue “wire-cage” inside the active centre pocket represented by the smooth surface.

Professor Davies was presented with the Roy L Whistler Award of the International Carbohydrate Organization at the XXIIIrd International Carbohydrate Symposium in Whistler in 2006.

© 2007 G. Davies. Published by Elsevier Ltd.

Available online at www.sciencedirect.com

Indexed/Abstracted in: Chem. Abstr.: Curr. Contents: Phys., Chem. & Earth Sci. Life Sci. Current Awareness in Bio. Sci (CABS). Full texts are incorporated in CJELSEVIER, a file in the Chemical Journals Online database which is available on STN® International. Also covered in the abstract and citation database SCOPUS®. Full text available on ScienceDirect®



ISSN 0008-6215